**RESEARCH ARTICLE**

# ECM stiffness regulates glial migration in *Drosophila* and mammalian glioma models

Su Na Kim[1], Astrid Jeibmann[2], Kathrin Halama[2], Hanna Teresa Witte[1,2], Mike Wälte[3], Till Matzat[1], Hermann Schillers[3], Cornelius Faber[4], Volker Senner[2], Werner Paulus[2] and Christian Klämbt[1,*]

## ABSTRACT

Cell migration is an important feature of glial cells. Here, we used the *Drosophila* eye disc to decipher the molecular network controlling glial migration. We stimulated glial motility by pan-glial PDGF receptor (PVR) activation and identified several genes acting downstream of PVR. *Drosophila lox* is a non-essential gene encoding a secreted protein that stiffens the extracellular matrix (ECM). Glial-specific knockdown of Integrin results in ECM softening. Moreover, we show that *lox* expression is regulated by Integrin signaling and vice versa, suggesting that a positive-feedback loop ensures a rigid ECM in the vicinity of migrating cells. The general implication of this model was tested in a mammalian glioma model, where a Lox-specific inhibitor unraveled a clear impact of ECM rigidity in glioma cell migration.

KEY WORDS: **Drosophila, Human, Mouse, Glial cell migration, PVR, PDGF-receptor, Lysyl oxidase, *Lox*, Extracellular matrix**

## INTRODUCTION

The formation of the brain is one of the most fascinating processes in development. Once neurons are born, they settle and never divide again. By contrast, glial cells retain mitogenic and motile properties. Glial motility requires intensive interaction with the extracellular environment. On the one hand directional cues have to be perceived; on the other hand, a dynamic regulation of cell-cell or cell-matrix contact is needed to allow glial migration (Friedl and Gilmour, 2009; Klämbt, 2009).

In *Drosophila*, glial migration has been extensively studied in several parts of the nervous system (Klämbt, 2009). During embryogenesis, peripheral glia migration is in part controlled by Netrin signaling and the modulation of adhesive forces is provided by the expression of the NCAM homolog Fasciclin2 (von Hilchen et al., 2010; Sepp et al., 2000; Silies and Klämbt, 2010; Silies and Klämbt, 2011). During larval development, the forming visual system provides an easily accessible model system with which to study glial migration. Photoreceptor neurons emerge in the eye imaginal disc (eye disc), which is connected to the brain by the optic stalk. All retinal glial cells are derived from the optic stalk glia and subsequently move onto the eye disc (Choi and Benzer, 1994; Rangarajan et al., 1999; Silies et al., 2007b). The proliferation and subsequent differentiation is controlled by a sequential activation of the fibroblast growth factor (FGF) receptor and only the sustained

overactivation of the FGF receptor leads to the formation of massive solid tumors (Franzdóttir et al., 2009). Whereas FGF-receptor activity promotes glial proliferation, activity of Neurofibromin2 counteracts glial proliferation in flies as well as in human neurofibromatosis (Asthagiri et al., 2009; Reddy and Irvine, 2011).

Owing to the inherent mitogenic potential of glia, glial tumors are common in humans and gliomas are among the most deadly types of cancer (Furnari et al., 2007). The most aggressive form is glioblastoma [World Health Organization (WHO) grade IV], an astrocytic tumor with a median survival of 16 months (Furnari et al., 2007). Owing to their highly invasive nature, glioblastomas cannot be completely resected, and even though multimodal therapeutic approaches comprising surgical resection followed by radiation and chemotherapy are applied, prognosis is dismal. In recent years, a number of molecular pathways contributing to glioma formation have been identified (Riemenschneider et al., 2010; Verhaak et al., 2010). Amplification of the epidermal growth factor (EGF) receptor occurs in 40% of all glioblastomas and contributes to glial proliferation (Libermann et al., 1985; Louis et al., 2007). Platelet-derived growth factor (PDGF) receptor pathway activation via genomic amplification or overexpression is often linked to glioma progression and worse prognosis (Brennan et al., 2009; Ozawa et al., 2010). Accordingly, inhibitors of the PDGF receptor pathway, such as imatinib or dasatinib, are clinically explored in individuals with glioblastoma (Morris and Abrey, 2010; Paulsson et al., 2011).

Here, we have employed a *Drosophila* glioma model (Read et al., 2009; Witte et al., 2009) where glial cell motility is evoked by activation of the PDGF receptor homolog PVR. Cell migration is in part regulated by extracellular matrix (ECM) stiffness, which is mediated through Lysyl oxidase (Lox) activity. *Drosophila* encodes two genes with such enzymatic activity (Molnar et al., 2005). Both genes appear to be regulated through PVR and PVR is not able to evoke ectopic glial migration when their function is removed. We use atomic force microscopy (AFM) to show that *Drosophila* Lox regulates the stiffness of the ECM. Moreover, we demonstrate a positive-feedback loop via Integrin signaling that ensures a rigid ECM in the vicinity of migrating cells. We further use a mouse xenograft model: following transplantation, glioma cells rapidly colonize the host brain; this colonization is suppressed when Lox activity is blocked by a specific inhibitor. Our results highlight the relevance of ECM rigidity in the modulation of glioma cell migration and suggest novel therapeutic targets.

## RESULTS

### The *Drosophila* PDGF/VEGF receptor homolog stimulates glial migration

During *Drosophila* eye development, photoreceptor neurons develop in the eye disc, whereas retinal glial cells are born in the CNS and migrate onto the eye disc through the so-called optic stalk

[1]Institute of Neurobiology, University of Münster, Münster 48149, Germany. [2]Institute of Neuropathology, University Hospital Münster, Münster 48149, Germany. [3]Institute of Physiology II, University Hospital Münster, Münster 48149, Germany. [4]Department of Clinical Radiology, University Hospital Münster, Münster 48149, Germany.

*Author for correspondence (klaembt@uni-muenster.de)

DEVELOPMENT

(Fig. 1A,C). At the end of larval development, about 350 glial cells populate every eye disc (Silies et al., 2007b).

Glial expression of activated PVR (λPVR), the *Drosophila* PDGF- and VEGF-receptor homolog, resulted in increased migration with streams of glial cells moving across the eye disc in young third instar larvae (Figs 1 and 3). In addition, we noted a reduction in glial cell number (15%, *n*=30 discs) and an increase in the size of glial nuclei (57%, *n*>200 cells). Depending on the migration pattern, we defined three different phenotypic classes (Fig. 1). In about 50% of the eye discs (*n*=43) we observed streams of glial cells on both the basal and the apical side of the eye disc (Fig. 1D). In 40% we noted glial migration along the Bolwig's nerve on the peripodial membrane of the eye imaginal disc, whereas in the remaining discs abnormal glial migration was noted on the basal side (Fig. 1E,F).

Pan-glial expression of activated FGF receptor results in dramatically increased glial number, but does not induce glial migration (Franzdóttir et al., 2009). Thus, signaling downstream of receptor tyrosine kinases diverts either to promote cell division or to stimulate cell migration. PVR-induced cell migration is manifested already very early in development and can be seen in second instar larvae (supplementary material Fig. S1A,B). In addition, concomitant misprojections of the photoreceptor axons are seen in ~40% of the eye discs dissected from third instar larvae (*n*=23, supplementary material Fig. S1C,D). Within the brain, glial cells expressing activated PVR are organized in an abnormal multilayered fashion (supplementary material Fig. S1E,F). Importantly, PVR signaling appears to primarily instruct cell migration. However, phenotypes were only apparent when animals were grown at 18°C, whereas a culture temperature of 25°C resulted in embryonic/early larval lethality.

## RNAi screen to identify cell-autonomously acting components required for glial migration

To further understand how PVR activity is transduced to increase cell motility, we followed a genetic approach and screened for genes that would alleviate the consequences of PVR over-activation by using a cell-type-specific knockdown of gene functions via Gal4-mediated expression of dsRNA (Dietzl et al., 2007). We generated a tester fly strain in which the Gal4-mediated expression of activated PVR is blocked by concomitant ubiquitous Gal80 expression {*UAS-λPVR/UAS-λPVR; repo-Gal4 UAS-CD8GFP/TM6 tub-Gal80*}. When these tester flies are crossed to wild-type flies, Gal80 function is removed genetically (supplementary material Fig. S2) and all non-TM6 flies, which can be recognized by the dominant marker Tubby, die due to the activation of PVR mediated by *repo*-Gal4 activity in glial cells.

We next crossed the tester flies to flies carrying different *UAS-dsRNA* constructs. The non-TM6 progeny of these crosses were then scored for a shift in the lethal phase towards pupal stages. Following screening of 2000 lines, we identified several genes that, upon silencing, shifted the lethal phase to late third instar or even pupal stages (Table 1). Silencing of PVR function in this paradigm also shifts the lethal phase to the pupal stage and serves as a control in the screen. We noted a shift in lethal phase upon silencing several components of the *hedgehog* signaling pathway, which has previously been associated with glial migration (Rangarajan et al., 2001) (Table 1). Hedgehog binding to Patched blocks its negative action on Smoothened (Briscoe and Thérond, 2013; Ingham et al., 2011) and thus it was surprising that knockdown of *hedgehog* or *patched* both shift the early lethality induced by glial PVR expression. In agreement with these findings, we were able to rescue the early lethal phenotype of PVR expression upon panglial co-expression of Patched. We also identified several members of the RTK and Wingless signaling pathways. The largest group of genes affecting PVR-induced lethality regulates transcription via chromatin regulation (Table 1). The strongest suppression effects were noted upon silencing of *Bap60* and *lox* (Table 1). As *Bap60* might simply affect UAS-mediated PVR expression, we focused on an analysis of the role of *lox*.
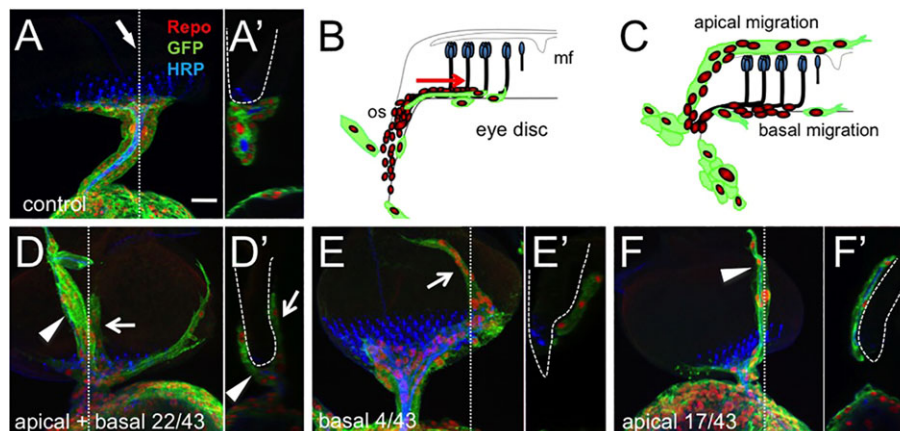


**Fig. 1. The activation of PVR signaling causes increased glial cell migration.** Larval eye discs attached to the brain stained for the glial nuclei marker Repo (red), for glial-expressed membrane-bound GFP (*repo*-Gal4 UAS-*CD8GFP*; green) and for the neuronal marker HRP (blue). Projections of confocal stacks are shown. (A′,D′,E′,F′) Orthogonal sections taken at the positions indicated by a dashed line in A,D,E,F. In the orthogonal views, the positions of the eye disc are indicated by a dashed curved line. (A) In young third instar *repo*-Gal4, UAS-*CD8GFP* larvae the normal distribution of glial cells is seen. The arrow indicates the end point of glial migration in the eye disc. (B) A young third instar eye disc. Glial migration is initiated at the optic stalk (os) and follows the differentiating photoreceptor axons (red arrow) in the wake of the morphogenetic furrow (mf). The eye disc is shown in an orthogonal view. (C) Glial migration following pan-glial activation of PVR. Glial cells are now frequently found on both sides of the eye disc. The eye disc is shown in an orthogonal view. (D-F) Eye imaginal discs of young third instar larvae of the genotype *repo*-Gal4, UAS-*CD8GFP UAS-λPVR*. (D,D′) In 22 out of 43 eye discs, we noted ectopic glial migration on both the apical and the basal side of the disc (the arrowhead indicates the apical migration stream; the arrow indicates the basal migration stream). (E,E′) In four out of 43 cases, we noted ectopic migration on the basal side of the eye imaginal disc (arrow). (F,F′) In 17 out of 43 cases, we noted ectopic migration along the Bolwig's nerve (arrowhead), which resides in the peripodial membrane. Scale bar: 20 μm.

**Table 1. Suppressor screen**

| CG | Gene | ID | Result | Molecular function grouped | Off targets |
|---|---|---|---|---|---|
| CG8222 | Pvr | 13502 | P | Signal transduction/receptor | – |
| CG15793 | Dsor1 | 40025 | L3 | Signal transduction/receptor | 1 |
| CG3166 | aop/Yan | BL26759 | L3 | Transcription | – |
| CG31163 | SKIP | 25702 | L3 | Signal transduction/receptor | – |
| CG11335 | lox | 11335R-3 | P | Cell adhesion/ECM | – |
| CG11335 | lox | Mutant | – | | |
| CG11335 CG4402 | lox lox2 | Double mutant | L3/P | | |
| CG2411 | patched | BL28795 | L3 | Signal transduction/receptor | – |
| CG4637 | hedgehog | BL31042‡ | L3 | Signal transduction/receptor | – |
| CG2125 | ci | BL31236‡ | L3 | Signal transduction/receptor | – |
| CG6407 | Wnt5 | BL28534 | L3 | Signal transduction/receptor | – |
| CG2621 | shaggy | BL31308 | L3 | Signal transduction/receptor | – |
| CG4636 | Wave | BL36121 | L3 | Cytoskeleton/scaffolding protein | – |
| CG15015 | Cip4 | BL31646 | L3 | Cytoskeleton/scaffolding protein | – |
| CG31256 | Brf | BL35623 | L3 | Transcription | – |
| CG7055 | dalao | BL26218 | L3 | Transcription | – |
| CG1064 | Snr1 | 108599 | L3/P | Transcription | – |
| CG3274 | Bap170 | 34581 | L3 | Transcription | – |
| CG4303 | Bap60 | 103634‡ | P | Transcription | – |
| CG31703 | CG31703 | 109981 | L3/P | Transcription | 2 |
| CG6502 | E(z) | BL31617* | L3 | Transcription | – |
| CG9495 | Scm | BL31614 | L3 | Transcription | – |
| CG12296 | klumpfuss | BL28731 | L3 | Transcription | – |
| CG9233 | fu2 | BL36631 | L3 | Transcription | – |
| CG4894 | Ca-α1D | 51491 | L3 | Transmembrane/transporter/channel | – |
| CG5802 | CG5802 | 6800 | L3/P | Transmembrane/transporter/channel | 1 |
| CG10738 | CG10738 | BL28580 | L3 | Signal transduction/receptor | – |

Following screening of 2000 UAS-dsRNA strains, we obtained the above list of constructs that are able to shift the lethal phase caused by expression of activated PVR in glial cells. The shift from early larval stages to either the third instar stage (L3) or pupal stage is indicated. The predicted molecular function is taken from FlyBase. For a few lines, off-targets are predicted. The ID numbers of Bloomington, VDRC or NIGFly are indicated. Genes are grouped according to their function.
*One additional line was tested with the identical results.
‡Two additional lines were tested with the identical results.

### lox-like genes act downstream of PVR

*lox* encodes a Lysyl oxidase, which in mammals is known to exert ECM crosslinking functions to increase ECM stiffness (Lucero and Kagan, 2006). Moreover, *lox* expression promotes breast cell metastasis, as increasing ECM stiffness promotes cell migration (Levental et al., 2009; Moore et al., 2010; Ng and Brugge, 2009).

In *Drosophila*, perineurial glial cells migrate below the neural lamella, a dense ECM surrounding the entire nervous system (Stork et al., 2008; Xie and Auld, 2011). We therefore set out to test whether modulation of ECM rigidity suppresses glial cell migration evoked by expression of activated PVR. A well-established specific inhibitor of Lox activity is BAPN (β-aminoproprionitrile). This small compound irreversibly blocks the catalytic properties of Lox family members (Smith-Mungo and Kagan, 1998; Tang et al., 1983). When we reared the flies on food containing 1.25 mM BAPN, we also noted a shift of the PVR-induced early larval lethality to late larval stages, with few animals reaching pupal stages (1-4 pupae/small vial with four females and two males; for crossing scheme, see supplementary material Fig. S2). This is never observed when PVR-overexpressing flies are fed untreated food, when lethality in early larval stages is found. This supports the notion that *lox* acts downstream of activated PVR and points towards the notion that *lysyl oxidase* function promotes migratory phenotypes evoked by PVR expression.

The *Drosophila* genome encodes two *lox*-related genes (Molnar et al., 2005). Whereas *lox* is weakly expressed throughout all developmental stages, *lox2* is expressed mostly in adults. Lox is a predicted 38.5 kDa large secreted protein, most closely related to the mammalian Loxl4 protein (Molnar et al., 2005, 2003) (Fig. 2A).

In *Drosophila* S2 cells, N- or C-terminally-tagged Lox protein of the predicted size is quantitatively found in the supernatant, suggesting that no proteolytic processing occurs in S2 cells (Fig. 2B,C). When we treated the supernatants with Endo H or PNGase F, which removes N-linked glycosylation, we noted only a slight change, indicating a moderate glycosylation of the protein (Fig. 2C). When we followed expression of a Myc-tagged Lox protein during *Drosophila* development in a ubiquitous manner using the *da*-Gal4 driver we found unprocessed secreted Lox protein in the larval hemolymph (Fig. 2D). Interestingly, we could also detect secreted Lox protein in the hemolymph when we expressed Lox specifically only in glial cells using the *repo*-Gal4 driver (Fig. 2D).

### lox-like genes suppress PVR-induced glial migration

To verify that *lox* plays a decisive role in regulating PVR-induced migration, we generated a *lox* mutant by imprecise excision of a P-element. In the allele *lox*$^{\Delta A38}$, the entire *lox*-coding sequence is removed without affecting the neighboring loci (supplementary material Fig. S3A). Flies homozygous for this mutation are viable and show no obvious external phenotypes. Likewise, the larval visual system forms with no discernible abnormalities (Fig. 3B). Moreover, pan-glial overexpression of *lox* does not interfere with normal glial migration (Fig. 2E,F).

Surprisingly, the *lox*$^{\Delta A38}$ mutation does not shift the lethal phase associated with glial expression of activated PVR. Given that the Lox inhibitor BAPN suppresses the PVR induced lethality, this may suggest that redundantly acting genes prevent a phenotypic rescue. The deduced Lox2 protein is highly related to the Lox protein in
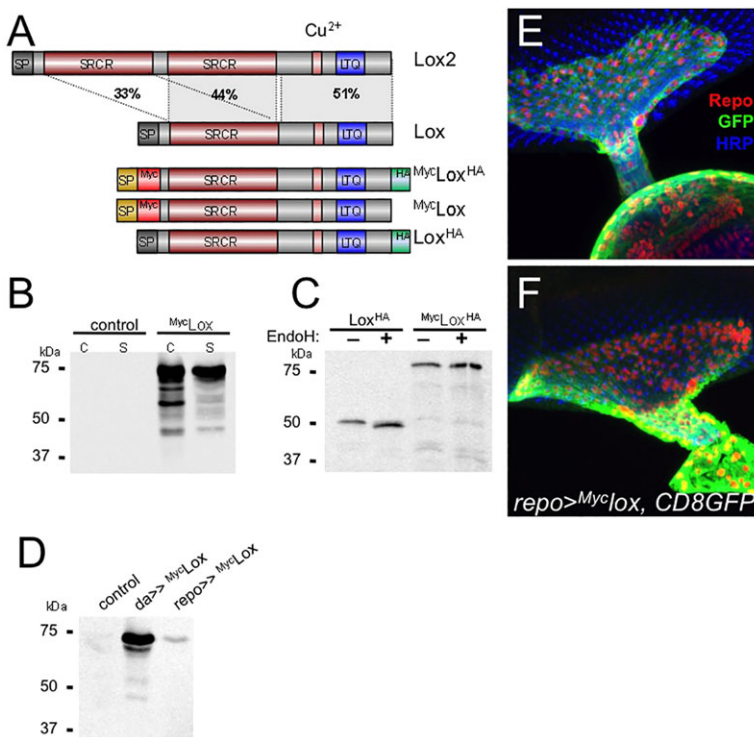
**Fig. 2. Molecular analysis of *Drosophila* lox.** (A) The *Drosophila* Lox-like proteins. Lox2 is structurally similar to Lox. SP, signal peptide; SRCR, scavenger receptor cysteine-rich domain; Cu²⁺, copper ion-binding site; LTQ, lysine tyrosylquinone co-factor. The numbers indicate the level of amino acid identity in the different domains. Three differentially tagged Lox protein variants are depicted. The two Myc-tagged Lox constructs contain a signal peptide derived from the Slit protein (yellow shading). (B) Western blot of protein extract generated from S2 cells probed for the expression of N-terminally Myc-tagged Lox. In untransfected cells (control), no Myc expression can be detected. In cells transfected with *actin*-Gal4 and UAS-*Myclox*, tagged Lox protein can be detected in cell extracts (c) and in the supernatant (s). (C) Western blot of protein extracts generated from S2 cells probed for expression of the HA epitope. Secreted proteins were treated (or not) with EndoH to remove N-linked glycosylation (–/+). (D) Western blot of the larval hemolymph. The Myc-tagged protein can be seen in the hemolymph following ubiquitous (*da*-Gal4) or pan-glial expression (*repo*-Gal4). (E,F) Third instar eye imaginal discs. Expression of CD8GFP in all glial cells is shown in green, glial nuclei are labeled in red, HRP staining is in blue. (E) Control animal with normal glial migration. (F) Upon overexpression of a Myc-tagged Lox, glial migration appears normal.

sequence (Fig. 2A). It carries two SRCR domains similar to the human Loxl2 protein (Molnar et al., 2005). A transposon induced *Drosophila lox2* mutation is available (supplementary material Fig. S3B). The transposon insertion disrupts the open reading frame and mostly likely removes the catalytic function of Lox2. *lox2* mutants are fertile and no abnormal phenotypes were detected in the eye disc. By contrast, *lox lox2* double mutant animals are male sterile but no defects in glial migration onto the eye imaginal disc were noted (*n*=13, Fig. 3C). However, we noted that the optic stalk is shortened and thicker in 50% of the cases (7/13). To demonstrate this phenotype, we analyzed intact third instar brains with the eye imaginal disc attached. In a single confocal section, this tubby-like optic stalk phenotype can be identified (Fig. 3C′, arrows). These phenotypes suggest at least partially redundant functions of *lox* and *lox2*.

When activated PVR is expressed in a *lox lox2* double mutant background, the lethal phase is shifted to late larval stages with rare animals reaching pupal stages, as observed following BAPN treatment (see above). Importantly, the glial overmigration caused by expression of activated PVR onto the eye disc is suppressed (Fig. 3D,E, *n*=7). In addition, the optic stalk appears thicker than normal, resembling that of *lox lox2* double mutants (Fig. 3C′,E). In agreement with these observations, we found that *lox* and *lox2* mRNA expression is regulated by PVR activity. Interestingly, activated PVR is able to induce *lox* expression during embryogenesis, whereas *lox2* expression is activated only in larval tissues (Table 2).

### Lox is required for stiffness of the extracellular matrix

Lox oxidizes peptidyl lysine residues to α-aminoadipic-δ-semialdehyde (e.g. of collagen), which permits covalent cross-linking and thus *lox* genes are crucial for ECM maturation (Lucero and Kagan, 2006). In humans, *cutis laxa*, a rare congenital disorder, is associated with *lox* deficiency and is characterized by a lack of collagen monomer cross-linking, which affects the elasticity and thus the rigidity of the ECM. In breast cancer, *lox* dysfunction has been implicated in metastasis (Leventhal et al., 2009).

During *Drosophila* eye development, glial cells migrate along a thick ECM called neural lamella (Silies et al., 2007b). We therefore assayed the elastic properties of the ECM in an area of the eye disc that is contacted by migrating glia using atomic force microscopy (AFM; Fig. 4A). The force required to indent the AFM tip about 200 nm into the neural lamella was measured and Young's modulus, which describes the elasticity of the matrix, was calculated.

In wild type, Young's modulus is around 400 Pa (median 384; mean 426, both values are indicated; *n*=488 independent measurements in ten imaginal discs; Fig. 4B,C, all measurements are summarized in supplementary material Table S1). A pronounced reduction in rigidity was noted in flies homozygous for the excision allele $lox^{\Delta A438}$ (222; 221; *n*=165, four imaginal discs; Fig. 4C). By contrast, pan-glial overexpression of *lox* resulted in increased rigidity in the overlying ECM (431; 522; *n*=170, four imaginal discs; Fig. 4C) when compared with wild-type or *repo*-Gal4 control imaginal discs.

Given the decrease in ECM stiffness noted in *lox* mutants, we analyzed the ultrastructure of the neural lamella in wild type and *lox* mutants by transmission electron microscopy. The ECM generated in *lox* mutants appeared structurally similar to the wild-type ECM. When we analyzed the ECM of *lox* and *lox lox2* mutant larvae, we noted no significant increase in its thickness. Areas with reduced and increased ECM thickness are found in about equal numbers (Fig. 4D-G, arrows). For quantification, we determined the actual size of the ECM at 24 positions per optic stalk, defined by randomly placing a star on the TEM image and measuring the thickness of the ECM at the respective intersections (Fig. 4H,I). The ECM thickness varies from 150 nm to 700 nm (*n*=5 optic stalks per genotype). In summary, this shows that ECM rigidity, but not its apparent structure, is crucially regulated by *lox*.

### Integrin signaling establishes a positive-feedback loop to increase ECM stiffness

Most cell-matrix interactions are mediated by Integrin receptors and we therefore asked whether the rigidity of the ECM is

DEVELOPMENT
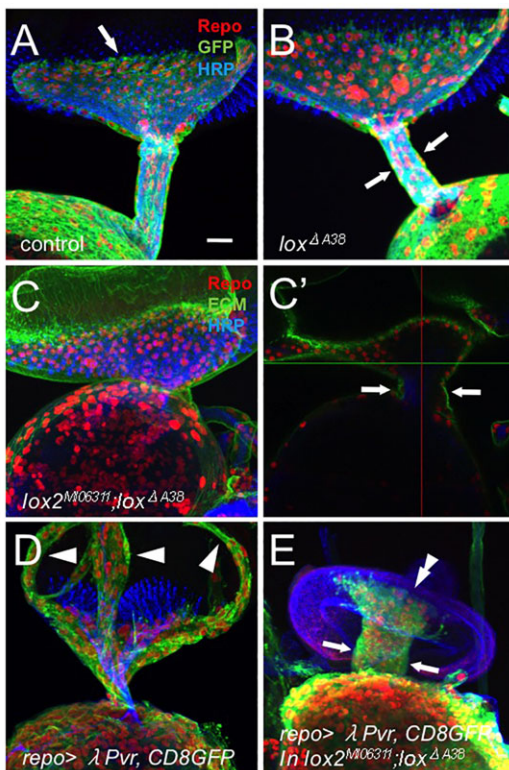
**Fig. 3. Loss of *lox* activity suppresses the glial migration induced by PVR activation.** Eye discs are stained as described in Fig. 1. (A) In mature eye discs, glial migration stops at the position where photoreceptor axons are formed (arrow). (B) Eye disc of a homozygous *Df(3R)lox*$^{\Delta A38}$ larva. (C,C′) Fifty percent of the *lox*$^{\Delta A38}$ *lox2*$^{MI06311}$ double mutant eye discs exhibit a shorter and broader optic stalk. The shape of the tissue was labeled using anti-Nidogen (Ndg) antibodies. (C′) Single confocal section. (D) Pan-glial activation of PVR (*repo*-Gal4; UAS-$\lambda$*Pvr*) leads to ectopic migration of glial cells (arrowhead). (E) In UAS-$\lambda$*Pvr lox2*$^{MI06311}$/*lox2*$^{MI06311}$; *repo*-Gal4 UAS-*CD8GFP lox*$^{\Delta A38}$/*lox*$^{\Delta A38}$ double mutant eye discs, migration appears normal (double arrowhead). (B,C′,E) The arrows indicate the optic stalk. Scale bar: 20 µm.

also influenced by integrins. Glial-specific knockdown of *myospheroid* encoding a β-Integrin subunit also resulted in a softer more-flexible matrix, demonstrating that Integrin signaling not only mediates the adhesion to the ECM but also signals towards the regulation of matrix rigidity (184; 211; *n*=42; two imaginal discs; Fig. 4C). In addition, pan-glial suppression of *myospheroid* expression by RNAi suppressed migration of glial cells onto the eye disc (supplementary material Fig. S4). A similar reduction in ECM stiffness was noted in mutants lacking the *focal adhesion kinase* (*fak*), which is involved in integrin signaling (178; 327; *n*=205; six imaginal discs; Fig. 4C). However, glial migration onto the eye disc does not appear to be affected. Moreover, when we co-expressed the *Drosophila* integrins PS1 and PS2 [*multiple edematous wings* (*mew*) and *inflated* (*if*)] in glial cells, the overlying ECM turned stiffer (411; 479; *n*=225; seven imaginal discs; Fig. 4C).

The modulation of ECM stiffness in response to Integrin signaling prompted us to determine a possible link between *integrin* and PVR function. PVR activation significantly induces expression of *myospheroid* (Table 2), but silencing of *myospheroid* did not suppress the lethal phenotype induced by PVR expression. However, overexpression of Integrin causes an upregulation of *lox* and *lox2* expression predominantly in the larvae, whereas overexpression of *lox* causes an upregulation of *myospheroid*

**Table 2. Relative expression of *lox*, *lox2* and *mys***

| Age/tissue | Genotype | *lox* | *lox2* | *mys* |
|---|---|---|---|---|
| Stage 14-16 whole embryo | *repo> CD8GFP* | 1.000 | 1.000 | 1.000 |
| | *repo> λPvr, CD8GFP* | 1.751** | 0.656** | 2.395** |
| | *2x repo> Integrin, CD8GFP* | 1.741*** | 0.618*** | 1.651** |
| Early third instar larval CNS | *repo> CD8GFP* | 1.000 | 1.000 | 1.000 |
| | *repo> λPvr, CD8GFP* | 0.272** | 7.464** | 14.689** |
| Third instar larval CNS | *w*$^8$ | 1.000 | ND | 1.000 |
| | *lox*$^{\Delta A38}$ | 0.000*** | ND | 0.714*** |
| | *Fak*$^{CG1}$ | 0.440** | 4.9*** | 0.839*** |
| | *2x repo> CD8GFP* | 1.000 | 1.000 | 1.000 |
| | *2x repo> Integrin, CD8GFP* | 3.706*** | 25.723*** | 7.621* |
| | *2x repo>* $^{Myc}$*lox, CD8GFP* | 85.430*** | 5.809*** | 18.722* |

Summary of the relative expression data of *lox*, *lox2* and *myospheroid* (*mys*) as determined by qRT-PCR normalized to expression of *rp49*. The relevant genotypes, the tissues analyzed and the *P*-values are indicated (**P*<0.1, ***P*<0.01, ****P*<0.001). *repo*, *repo-Gal4*; *2x repo*, two copies of *repo-Gal4*. All experiments were repeated at least three times. In embryos, expression of activated PVR causes an elevation of *lox* and *mys* expression. *lox2* expression is slightly reduced. By contrast, in young third instar larvae, *lox* expression is reduced, whereas *lox2* and *mys* expression is increased. Owing to the lethal effect of PVR expression, this experiment could not be performed in late third instar larvae. Upon overexpression of integrin subunits, we detected an increase of *lox* expression in the whole embryo and in the CNS of late third instar larvae. *lox2* expression is normally not detected in the CNS of late larval third instar (ND). Upon expression of *integrin* or *lox*, however, we detected *lox2* expression. We also noted an increase in *mys* expression when we overexpressed *lox*, and a slight decrease in *mys* expression in the CNS of *lox* mutants.

expression (Table 2). These data suggest that a feedback loop is established that ensures the stiff extracellular matrix of actively migrating cells (see Discussion).

**Lox inhibition restricts glioma cell migration**

The above data demonstrate the crucial role of ECM modulation during glial migration in response to PVR activation in *Drosophila*. Because, in humans, PDGF receptor activation is often linked to glioma progression and to a worse prognosis (Brennan et al., 2009; Ozawa et al., 2010), we analyzed the expression of human LOX genes. The human genome encodes *LOX* and four members of the LOX-like family (Lucero and Kagan, 2006; Molnar et al., 2003). *LOX*, *LOXL1* and *LOXL4* are expressed in the normal brain, where they are found mostly in neurons, vessel walls and some glia of the white matter (Fig. 5A-C). In glioblastoma biopsy tissue, however, an increase of LOX, LOXL1 and LOXL4 expression is detected (*n*=17 patients, Fig. 5D-F). In addition, we noted expression of LOX genes in different glioblastoma cell lines (human glioma cell lines U343 and A172 or rat C6-SPGFP cells; Fig. 5G-J).

As glioma cells are able to secrete extracellular matrix components (Gladson, 1999), Lox expression by glioma cells in cell culture may be linked to their migration. To prove this hypothesis, we performed a scratch assay (see Materials and Methods). Following knockdown of expression of *LOXL4*, which is most similar to *Drosophila lox*, cell migration is slightly reduced (expression level about 12% in U343 and 5% in A172 cells after 24 h; and 15% after to 96 h of culture; Fig. 5K). However, when we
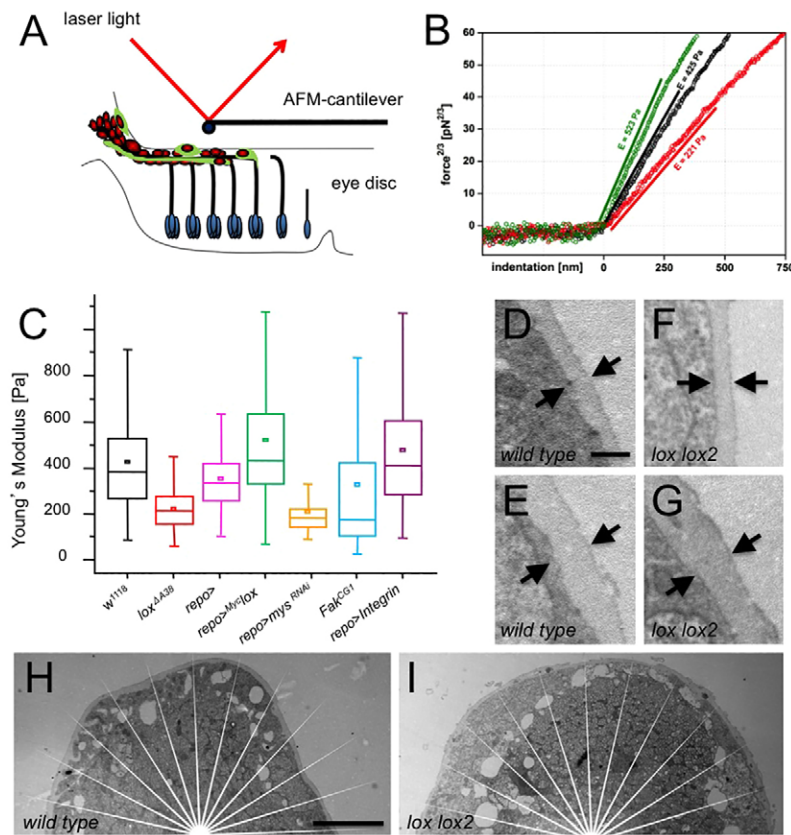
**Fig. 4. Lox affects ECM rigidity and structure.** (A) Principle of the AFM measurements of ECM elasticity. A spherical probe, mounted on a soft cantilever, indents the sample. The cantilever deflection, corresponding to the force, is detected by a laser beam that is reflected differentially from the reverse side of the cantilever. (B) Plot of three single force measurements. For calculation of the elasticity, see Materials and Methods. Wild type (425 Pa, black circles), *lox* mutant (221 Pa, red circles) and *lox* gain-of-function (523 Pa, green circles) are indicated. (C) Summary of the ECM elasticity data from wild-type and mutant *Drosophila* eye discs, the genotypes are indicated. The box plots indicate the median (line through the box) and the mean value (small square inside the box). (D,E) Two examples of wild-type ECM around the optic stalk shown in H. (F,G) Two examples of *lox lox2* double mutant ECM around the optic stalk shown in I. (H,I) TEM images of a cross-section through an optic stalk from a wandering wild-type (H) or *lox lox2* mutant (I) third instar larvae. Radial white lines indicate the positions at which we determined the thickness of the ECM. Scale bars: 0.5 µm in D-G; 5 µm in H,I.

stimulated U343 cell migration with 40 ng/ml PDGF-BB, relative migration was significantly decreased in the *LOXL4*-depleted cells (Fig. 5H). In conclusion, *lox*-like genes appear to have a function during cell migration in the mammalian system.

### Lox promotes tumor invasion *in vivo*
To directly test whether inhibition of the activity of the Lox-like enzymes also suppresses glioblastoma invasion, we then turned to a mouse xenograft model. The glioma cell line C6 is derived from a rat glioma and is widely used (Benda et al., 1968). To follow the C6 cells after stereotactic injection, we used the GFP expressing variant C6-SPGFP (Tatenhorst et al., 2005). C6-SPGFP cells ($4 \times 10^4$) were transplanted into identical positions of the striatum of female nude mice (*n*=10). Ten and 15 days later, tumor size was measured by MRI to document the increase in tumor volume (Fig. 6A,C). Subsequent histological analysis revealed extensive diffuse infiltration of GFP-positive C6 glioma cells into the host brain (Fig. 6D,F). In the transplanted C6-SPGFP cells, expression of *Loxl1* and *Loxl4* is upregulated compared with normal rat brain cells and can be easily detected (Fig. 6G,H,J). A similar upregulation of the expression of *lox*-family genes has been described for other astrocytoma cell lines (Laczko et al., 2007).

To test whether *lox* inhibition restricts migration of the rat glioma cells, as observed in the *Drosophila* model, we administered daily intraperitoneal doses of the Lox inhibitor BAPN (100 µg/g body weight in PBS), which also crosses the blood-brain barrier (Martin et al., 1991). A control cohort of mice was injected with PBS only. Mice injected with C6-SPGFP cells and daily BAPN doses developed gliomas that were indistinguishable from those in controls by MRI, with comparable proliferation indices (Fig. 6K,L). However, the extent of infiltration of glioma cells into the host brain was dramatically suppressed upon BAPN treatment (Fig. 6D,E).

A six- to sevenfold lower number of tumor cells or small tumor cell clusters was detected in the infiltration zone of BAPN-treated compared with control mice (*P*=0.008, Fig. 6F,I). In conclusion, BAPN inhibits glioma cell migration but does not affect tumor cell proliferation.

### DISCUSSION
Cell migration is of prime relevance during the development of the nervous system and is often triggered by the activation of the PDGF receptor. The *Drosophila* PDGF-receptor homolog PVR is required in a number of cell types for their normal migratory responses. In the fly ovary, *pvr* instructs the migration of border cells in part by influencing actin dynamics (Duchek et al., 2001; Fulga and Rørth, 2002; Rosin et al., 2004; Wang et al., 2006). In addition, migration of hemocytes and some embryonic glial cells depends on PVR activity (Cho et al., 2002; Janssens et al., 2010; Sears et al., 2003; Wood et al., 2006). In line with these findings, expression of activated PVR efficiently induces glial migration and generates phenotypes resembling a metastatic tumor cell phenotype (Vidal and Cagan, 2006; Witte et al., 2009). Likewise, PDGF-receptor activity instructs cell migration during normal mammalian development, but also during tumor metastasis (Hoch and Soriano, 2003; Jones and Cross, 2004; Shih and Holland, 2006).

Interestingly, the effects of activated PVR on glial motility appear to be a specific feature of this receptor tyrosine kinase, as activation of the related FGF-receptor results in extensive proliferation but does not trigger cell migration. Here, we used a genetic suppressor screen to better understand PVR-induced motility. We identified components of hedgehog and wingless signaling pathways. As both loss and gain of *patched* function is able to suppress the early lethality induced by PVR activation in glia, we suspect that the
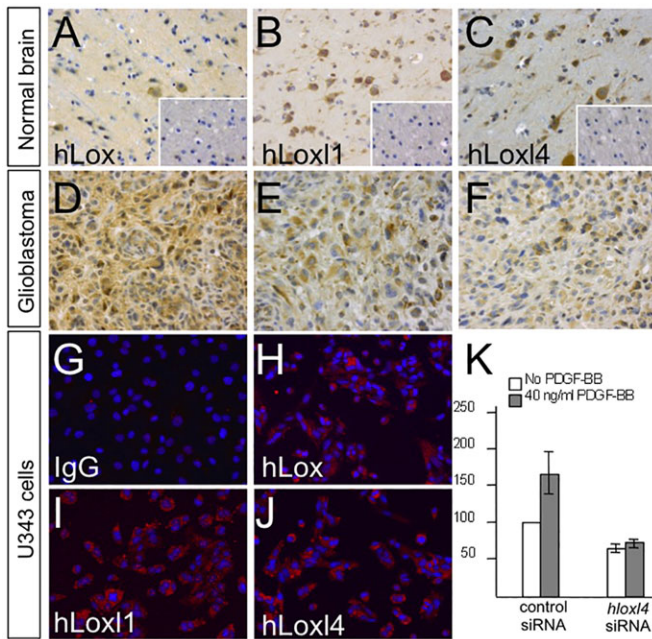
**Fig. 5. Upregulation and function of Lox proteins in human glioma cells.** (A-C) Expression of human LOX (A), LOXL1 (B) and LOXL4 (C) (brown) in autopsy cases is restricted to neurons, vessel walls and a few faintly positive glial cells of the white matter (insets). (D-F) Human glioblastoma biopsies stained for expression of LOX proteins. LOX (D), LOXL1 (E) and LOXL4 (F) were strongly expressed in human glioblastomas. Blue staining shows nuclei. (G-J) Expression of Lox proteins (red) in the cell line U343: IgG control (G), human LOX (H), LOXL1 (I) and LOXL4 (J). Nuclei are labeled by DAPI staining (blue). (K) Analysis of scratch assay. The relative migratory abilities of U343 cells were determined in relation to *LOXL4* expression and PDGF-BB treatment. Data are mean±s.e.m.

precise level of *hedgehog* signaling is crucially important during glial development. This might also account for the apparently different glial phenotypes associated with *hedgehog* (Hummel et al., 2002; Rangarajan et al., 2001).

Another component identified by our RNAi screen was *lox*. Surprisingly, we found that in contrast to the expression of *lox*[dsRNA], *lox* mutants do not suppress the PVR induced phenotype. As the Lox inhibitor BAPN is able to suppress PVR mediate lethality, we also analyzed the second *Drosophila* gene encoding a Lysyl oxidase (*lox2*). Recently, it was shown that Lox-mediated matrix stiffening also promotes breast and colorectal cancer metastasis (Baker et al., 2011; Levental et al., 2009). Increased ECM rigidity also favors migration of cultured glioma cells (Ulrich et al., 2009). In addition, we found that integrins affect the rigidity of the ECM, possibly by regulating *lox* mRNA expression. Thus, matrix rigidity often correlates with malignancy, suggesting more general implications of matrix rigidity and cell migration (Krndija et al., 2010; Paszek et al., 2005).

Cells exert forces during migration and thus favor a rigid surrounding (Moore et al., 2010). A number of receptors connect the cells to the ECM. Most prominent are members of the Integrin family, which not only provide mechanical coupling to the matrix, but also convey signals into the cell (Bökel and Brown, 2002; Ginsberg et al., 2005; Moore et al., 2010). The reduction in ECM stiffness following *myospheroid* knockdown or in *fak* mutants points to a role of Integrin signaling in regulating *lox* expression. Indeed, we observed an increase of *lox* expression in an Integrin gain-of-function situation (Table 2). Similarly, we noted a decrease in the level of *lox* mRNA expression in *fak* mutants. Thus, Lox and

Integrin might act in a positive-feedback loop enforcing a local extracellular environment favoring migration (Fig. 7).

In the mammalian system, integrins may suppress tumor metastasis (Ramirez et al., 2011). Generally, however, integrins are thought to be important mediators of cell adhesion and constitute attractive therapeutic targets to treat tumor progression (Weaver et al., 1997). In line with these findings, Integrin signaling is also key in regulating glioma cell migration (D'Abaco and Kaye, 2007; Fukushima et al., 1998). As BAPN can suppress glioma cell migration *in vivo*, this may indicate that the Lox/Integrin feedback loop identified in *Drosophila* is evolutionarily conserved to couple ECM stiffness to glioma cell migration.

The regulation of ECM stiffness via Lox is not required for viability. In humans, loss of *lox* leads to recessive connective tissue disorders (Smith-Mungo and Kagan, 1998), whereas no abnormal phenotypes were so far detected in *Drosophila* mutants (Molnar et al., 2005). In humans and *Drosophila*, *lox* activity is upregulated in wound repair (Smith-Mungo and Kagan, 1998; Stramer et al., 2008), reflecting the need for increased migration of cells into the wound area. Thus, Lox might be primarily involved in the regulation of plastic responses encountered during injury and disease.

Flies have a relatively simply structured nervous system; however, relatively few glial cells share pronounced motility with their mammalian counterparts (Klämbt, 2009). The *Drosophila* glioma model used here has disclosed a crucial role for Lox-related genes in maintaining the migratory state of mammalian glioma cells. Indeed, the cancer clinical genomics database 'Repository of Molecular Brain Neoplasia Data (Rembrandt)', which comprises a large number of glioma patient data (http://rembrandt.nci.nih.gov; Madhavan et al., 2009), demonstrates a significant correlation between the upregulation of *LOX* and *LOXL1* and overall survival. As BAPN treatment can block the diffuse infiltration of glioblastoma cells in a mouse model, new therapeutic strategies for a currently incurable disease might be in reach.

## MATERIALS AND METHODS
### Fly strains and genetics
All crosses were performed on standard food at 25°C unless indicated otherwise. The *lox*[ΔA438] excision mutant was generated from *P[XP]d09952*. The following strains were used: *repo*-Gal4, *repo4.3*-Gal4, UAS-*λhtl*, UAS-*λtop*, UAS-*λPvr*, UAS-*inflated* UAS-*mew* [ provided by V. Auld (University of British Columbia, Vancouver, Canada); B. Jones (University of Mississippi, Oxford, USA); M. Leptin (University of Cologne, Cologne, Germany); B. Shilo (Weizmann Institute, Rehovot, Israel); P. Rørth (University of Copenhagen, Copenhagen, Denmark); N. Brown (University of Cambridge, Cambridge, UK)]; *lox*[d09952] (Exelixis collection, Harvard University, Cambridge, USA); and *lox2*[MI06311], *tub>Gal80*, UAS-*CD8GFP*, *w*[1118] (Bloomington Stock Center, Bloomington, USA). UAS-dsRNA strains were from Bloomington, VDRC or NIGFly. For details see Table 1. The different tagged UAS-based *lox* transgenic fly strains were generated according to standard procedures.

### Molecular genetics
DNA cloning was conducted using Gateway-based vectors (Invitrogen). All constructs were verified by DNA sequencing. Proteins were extracted from cells and analyzed by western blot as described previously (Bogdan et al., 2005). For the glycosidase assay, proteins were extracted by TCA precipitation and deglycosylated by Endo H (Roche) or PNGase F (New England Biolabs) according to the manufacturer's instructions. We used RNase B as a positive control.

### Quantitative RT-PCR (qRT-PCR)
Total RNA was isolated from cultured cells or tissue with GenElute (Sigma-Aldrich) or TRizoL (Invitrogen). cDNA templates were synthesized using SUPERscript II polymerase with Oligo(dT)$_{12-18}$ primers and RNaseOUT
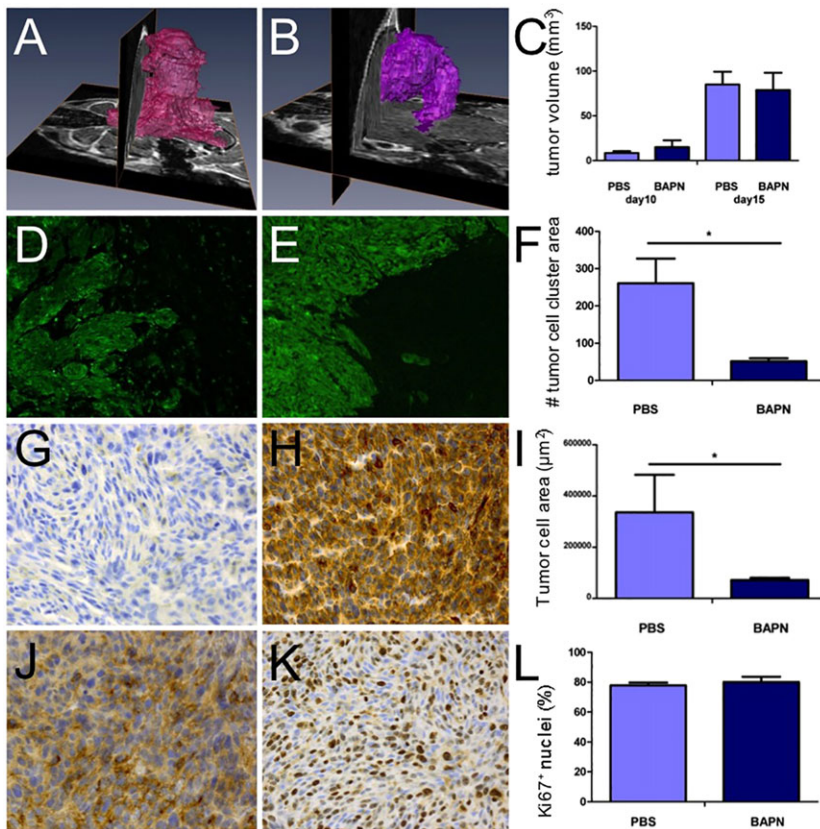
**Fig. 6. Inhibition of *Lox* function blocks infiltration of glioma cells.** (A,B) MRI 3D reconstruction of the tumor volume following injection of $10^4$ C6-SPGFP cells into the brain of PBS-treated (A) and BAPN-treated (B) mice. (C) Volumetric analysis revealed a similar increase in tumor volume between day 10 and day 15 in PBS- and BAPN-treated animals. (D) In PBS-treated animals, GFP-positive tumor cell clusters were detected in the infiltration zone. (E) Fewer glioma cells invaded into the brain of BAPN-treated animals. Quantification of number (F) and mean area (I) of tumor cell clusters in the infiltration zone. A significant reduction was seen in BAPN-treated mice (*$P$=0.008). (G,H,J) Expression of Lox family proteins in C6-SPGFP xenografts (brown). Lox was faintly expressed (G), whereas Loxl1 (H) and Loxl4 (J) were easily detected by immunostaining. (K,L) The proliferation index was determined using an antibody directed against rat Ki67 protein and was not significantly different in BAPN-treated (80.1%) versus PBS-treated (77.9%) mice ($P$=0.92). Data are mean±s.e.m.

(Invitrogen) following the manufacturer's instructions. qRT-PCR was performed using SYBR Green for monoplex reaction (Bioline), TaqMan Gene Expression Assays for duplex reaction (Applied Biosystems) and Realplex Mastercycler (Eppendorf) following the manufacturer's instructions. The analysis of the data was conducted using the REST 2009 software (Qiagen; Pfaffl et al., 2002). For primers see methods in the supplementary material.

### Elasticity measurements

Elasticity measurements were performed as described in a HEPES-buffered solution using a Nanoscope III Multimode-AFM (Veeco Instruments).



**Fig. 7. PVR induces a positive-feedback loop ensuring ECM stiffness and cell migration.** (A,B) Upon activation of PVR, expression of *integrin* (A) and *lox* (B) is induced (gray arrows). Lox is secreted (turquoise arrow) and crosslinks extracellular proteins to generate a more-rigid ECM. The stiff ECM is recognized by integrin receptors and favors migration. Integrin signaling then promotes *lox* expression (purple arrow), which sustains ECM stiffness on the migratory path of the cell.

Deflection of colloidal probe cantilevers with a sphere radius of 5 μm was determined and Young's modulus was calculated as follows:

$$E = \frac{3}{4}\left(\frac{\Delta(f)^{\frac{2}{3}}}{\Delta\delta}\right)^{\frac{3}{2}}\frac{1-v^2}{\sqrt{R}} = \frac{3}{4}slope^{\frac{3}{2}}\frac{1-v^2}{\sqrt{R}},$$
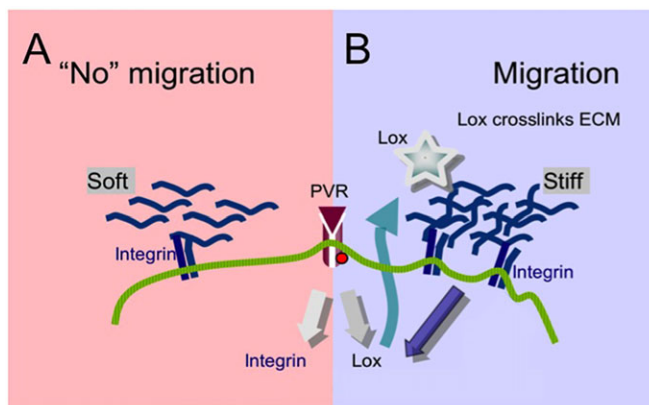
where $E$ is Young's modulus, $f$ is force ($f$), $v$ is Poisson ratio of the sample, $\delta$ is deformation or indentation depth, and $R$ is radius of the sphere. The initial part of the curves corresponding to indentation of 200 nm was analyzed using the linear implementation of equation 4 of the Hertz-Model. All force-indentation data were analyzed with PUNIAS (Protein Unfolding and Nano-Indentation Analysis Software, http://punias.voila.net/klmenu/punias0.htm), a custom-built semi-automatic processing and analysis software.

### Immunohistochemistry

Fixation and treatment of tissues for immunohistochemistry on third instar larval brains and eye imaginal discs were performed as described previously (Silies et al., 2007a; Stork et al., 2008). For a list of antibodies used, see methods in the supplementary material. LOX, LOXL1 and LOXL4 staining was evaluated semi-quantitatively by scoring the percentage of stained cells [0 (absent), 1 (<10%), 2 (10-50%), 3 (51-80%), 4 (81-100%)], as well as staining intensity [0 (absent), 1 (weak), 2 (strong)]. Both scores were multiplied resulting in a maximum staining score of eight.

### Scratch assay

U343 or A172 glioblastoma cells were transfected 1 day after plating using two siRNAi sequences (LOXL4_1 und LOXL4_4 siRNA, Qiagen) or control siRNA not able to bind known RNA sequences (AllStar negative siRNA, Qiagen). After 24 h the confluent cell layer was scratched with a sterile 100 μl pipette tip. The same area was documented after 0 h, 24 h, 48 h

and 72 h, and analyzed using 'analySIS FIVE' (Olympus) and TScratch software (ETH Zürich, Switzerland).

## Transmission electron microscopy

Fixation and sectioning was performed as described previously (Stork et al., 2008). All measurements were made using Photoshop. Five different animals were analyzed for each genotype.

## Human tissues

Glioblastomas (grade IV, WHO), obtained by biopsy (frozen, $n=10$; formalin-fixed and paraffin-embedded, $n=17$), and non-pathologic frontal lobe brain tissue, obtained by autopsy (frozen, $n=2$, formalin-fixed and paraffin-embedded, $n=2$), were examined. Ethical approval was obtained from the local Ethical Committee of the Ärztekammer Westfalen-Lippe, Germany (Az.2007-420-f-S).

## Xenotransplantation and BAPN-administration

C6-SP-GFP cells ($4 \times 10^4$ in 2 µl PBS) were transplanted into the right striatum of 20 anesthetized female NMRI nude mice (Elevage Janvier) aged 6 weeks using a stereotactic frame (Narashige). Cell suspensions were injected at 4 mm anterior to the interaural line, 2.5 mm lateral to the midline, at a depth of 3.5 mm into the brain. One day before transplantation, intraperitoneal injection of BAPN (100 µg/g/day in 50 µl of PBS) was started in 10 animals, while 10 control mice were injected with 50 µl of PBS. Intraperitoneal injection of BAPN or PBS was continued daily. On day 10 and day 15, MRI was carried out. At day 15 after injection, brains were prepared. Five brains of each group were immediately frozen in liquid nitrogen, while five brains of each group were fixed in formalin and embedded in paraffin. Ethical approval was obtained from the local Ethical Committee of the Ärztekammer Westfalen-Lippe, Germany (Az.2007-420-f-S).

## MRI

MRI measurements were performed on a 3T Philips Achieva System. A 3D gradient echo dataset was acquired in 8.50 min scan time using SPIR fat suppression and the following parameters: isotropic resolution, 200 µm; reconstructed to $90 \times 90 \times 200$ µm$^3$; field of view (FOV), $20 \times 14 \times 8$ mm$^3$; echo time/repetition time (TE/TR), 5.5/28 ms; excitation pulse angle, 35°; averages, 6. As contrast agent, Gd-DTPA (Magnevist) was applied at 0.5 mmol/kg body weight through a tail vein catheter 5 min prior to measurement start. Hyperintense-appearing tumor tissue was segmented semi-manually using Amira (Visage Imaging) and the volume was calculated.

## Morphometry

Serial coronal sections (3 µm) were made from paraffin-embedded brain tissue of xenotransplanted mice ($n=5$ for BAPN and control mice). Whole sections were photographed using an automated Corvus high resolution stage control. Areas of tumor core and infiltration zone were quantified using Analysis software and a fixed threshold of light intensity. Fluorescent cell clusters detected outside the tumor core were investigated with respect to size (µm$^2$) and number. We used ImageJ to determine the nuclear sizes. In wild type, almost all glial nuclei appeared round. By contrast, glial nuclei appeared more oval upon expression of activated PVR. The longest diameter of a glial nucleus was measured in ImageJ and was taken as size value.

## Statistics

Comparison of tumor volume (MRI investigation) was analyzed using two-way ANOVA [treatment as between-subject factor and timepoints (10 days and 15 days after implantation) as within-subject factor]. Number of GFP-positive tumor cell clusters in the infiltration zone was compared by Mann–Whitney $U$-test. Results of the migration assay were analyzed by Student's $t$-test. $P<0.05$ was considered significant. Experiments were performed independently three times. All statistical analyses were performed using IBM SPSS Statistics 18 version 18.0.

## Author contributions

S.N.K. designed the work and performed the *Drosophila* experiments; A.J. designed the work and performed the mammalian immunohistochemistry and xenograft experiments; K.H. performed the scratch assay; H.T.W. established the *Drosophila* strains used in this work and performed the initial experiments; M.W. performed the AFM experiments; T.M. performed the TEM analysis; H.S. analyzed the AFM data; C.F. performed the MRI measurements; V.S. participated in the xenograft experiments; W.P. designed experiments; C.K. designed experiments and wrote the manuscript.

## Supplementary material

Supplementary material available online at
http://dev.biologists.org/lookup/suppl/doi:10.1242/dev.106039/-/DC1

## References

**Asthagiri, A. R., Parry, D. M., Butman, J. A., Kim, H. J., Tsilou, E. T., Zhuang, Z. and Lonser, R. R.** (2009). Neurofibromatosis type 2. *Lancet* **373**, 1974-1986.

**Baker, A.-M., Cox, T. R., Bird, D., Lang, G., Murray, G. I., Sun, X.-F., Southall, S. M., Wilson, J. R. and Erler, J. T.** (2011). The role of lysyl oxidase in SRC-dependent proliferation and metastasis of colorectal cancer. *J. Natl. Cancer Inst.* **103**, 407-424.

**Benda, P., Lightbody, J., Sato, G., Levine, L. and Sweet, W.** (1968). Differentiated rat glial cell strain in tissue culture. *Science* **161**, 370-371.

**Bogdan, S., Stephan, R., Löbke, C., Mertens, A. and Klämbt, C.** (2005). Abi activates WASP to promote sensory organ development. *Nat. Cell Biol.* **7**, 977-984.

**Bökel, C. and Brown, N. H.** (2002). Integrins in development: moving on, responding to, and sticking to the extracellular matrix. *Dev. Cell* **3**, 311-321.

**Brennan, C., Momota, H., Hambardzumyan, D., Ozawa, T., Tandon, A., Pedraza, A. and Holland, E.** (2009). Glioblastoma subclasses can be defined by activity among signal transduction pathways and associated genomic alterations. *PLoS ONE* **4**, e7752.

**Briscoe, J. and Thérond, P. P.** (2013). The mechanisms of Hedgehog signalling and its roles in development and disease. *Nat. Rev. Mol. Cell Biol.* **14**, 418-431.

**Cho, N. K., Keyes, L., Johnson, E., Heller, J., Ryner, L., Karim, F. and Krasnow, M. A.** (2002). Developmental control of blood cell migration by the Drosophila VEGF pathway. *Cell* **108**, 865-876.

**Choi, K.-W. and Benzer, S.** (1994). Migration of glia along photoreceptor axons in the developing Drosophila eye. *Neuron* **12**, 423-431.

**Dietzl, G., Chen, D., Schnorrer, F., Su, K.-C., Barinova, Y., Fellner, M., Gasser, B., Kinsey, K., Oppel, S., Scheiblauer, S. et al.** (2007). A genome-wide transgenic RNAi library for conditional gene inactivation in Drosophila. *Nature* **448**, 151-156.

**Duchek, P., Somogyi, K., Jékely, G., Beccari, S. and Rørth, P.** (2001). Guidance of cell migration by the Drosophila PDGF/VEGF receptor. *Cell* **107**, 17-26.

**D'Abaco, G. M. and Kaye, A. H.** (2007). Integrins: molecular determinants of glioma invasion. *J. Clin. Neurosci.* **14**, 1041-1048.

**Franzdóttir, S. R., Engelen, D., Yuva-Aydemir, Y., Schmidt, I., Aho, A. and Klämbt, C.** (2009). Switch in FGF signalling initiates glial differentiation in the Drosophila eye. *Nature* **460**, 758-761.

**Friedl, P. and Gilmour, D.** (2009). Collective cell migration in morphogenesis, regeneration and cancer. *Nat. Rev. Mol. Cell Biol.* **10**, 445-457.

**Fukushima, Y., Ohnishi, T., Arita, N., Hayakawa, T. and Sekiguchi, K.** (1998). Integrin alpha3beta1-mediated interaction with laminin-5 stimulates adhesion, migration and invasion of malignant glioma cells. *Int. J. Cancer* **76**, 63-72.

**Fulga, T. A. and Rørth, P.** (2002). Invasive cell migration is initiated by guided growth of long cellular extensions. *Nat. Cell Biol.* **4**, 715-719.

**Furnari, F. B., Fenton, T., Bachoo, R. M., Mukasa, A., Stommel, J. M., Stegh, A., Hahn, W. C., Ligon, K. L., Louis, D. N., Brennan, C. et al.** (2007). Malignant astrocytic glioma: genetics, biology, and paths to treatment. *Genes Dev.* **21**, 2683-2710.

**Ginsberg, M. H., Partridge, A. and Shattil, S. J.** (2005). Integrin regulation. *Curr. Opin. Cell Biol.* **17**, 509-516.

**Gladson, C. L.** (1999). The extracellular matrix of gliomas: modulation of cell function. *J. Neuropathol. Exp. Neurol.* **58**, 1029-1040.

**Hoch, R. V. and Soriano, P.** (2003). Roles of PDGF in animal development. *Development* **130**, 4769-4784.

Hummel, T., Attix, S., Gunning, D. and Zipursky, S. L. (2002). Temporal control of glial cell migration in the Drosophila eye requires gilgamesh, hedgehog, and eye specification genes. Neuron 33, 193-203.

Ingham, P. W., Nakano, Y. and Seger, C. (2011). Mechanisms and functions of Hedgehog signalling across the metazoa. Nat. Rev. Genet. 12, 393-406.

Janssens, K., Sung, H.-H. and Rørth, P. (2010). Direct detection of guidance receptor activity during border cell migration. Proc. Natl. Acad. Sci. USA 107, 7323-7328.

Jones, A. V. and Cross, N. C. P. (2004). Oncogenic protein tyrosine kinases. Cell. Mol. Life Sci. 61, 2912-2923.

Klämbt, C. (2009). Modes and regulation of glial migration in vertebrates and invertebrates. Nat. Rev. Neurosci. 10, 769-779.

Krndija, D., Schmid, H., Eismann, J.-L., Lother, U., Adler, G., Oswald, F., Seufferlein, T. and von Wichert, G. (2010). Substrate stiffness and the receptor-type tyrosine-protein phosphatase alpha regulate spreading of colon cancer cells through cytoskeletal contractility. Oncogene 29, 2724-2738.

Laczko, R., Szauter, K. M., Jansen, M. K., Hollosi, P., Muranyi, M., Molnar, J., Fong, K. S. K., Hinek, A. and Csiszar, K. (2007). Active lysyl oxidase (LOX) correlates with focal adhesion kinase (FAK)/paxillin activation and migration in invasive astrocytes. Neuropathol. Appl. Neurobiol. 33, 631-643.

Levental, K. R., Yu, H., Kass, L., Lakins, J. N., Egeblad, M., Erler, J. T., Fong, S. F. T., Csiszar, K., Giaccia, A., Weninger, W. et al. (2009). Matrix crosslinking forces tumor progression by enhancing integrin signaling. Cell 139, 891-906.

Libermann, T. A., Nusbaum, H. R., Razon, N., Kris, R., Lax, I., Soreq, H., Whittle, N., Waterfield, M. D., Ullrich, A. and Schlessinger, J. (1985). Amplification, enhanced expression and possible rearrangement of EGF receptor gene in primary human brain tumours of glial origin. Nature 313, 144-147.

Louis, D. N., Ohgaki, H., Wiestler, O. D., Cavenee, W. K., Burger, P. C., Jouvet, A., Scheithauer, B. W. and Kleihues, P. (2007). The 2007 WHO classification of tumours of the central nervous system. Acta Neuropathol. 114, 97-109.

Lucero, H. A. and Kagan, H. M. (2006). Lysyl oxidase: an oxidative enzyme and effector of cell function. Cell. Mol. Life Sci. 63, 2304-2316.

Madhavan, S., Zenklusen, J.-C., Kotliarov, Y., Sahni, H., Fine, H. A. and Buetow, K. (2009). Rembrandt: helping personalized medicine become a reality through integrative translational research. Mol. Cancer Res. 7, 157-167.

Martin, J. E., Sosa-Melgarejo, J. A., Swash, M., Mather, K., Leigh, P. N. and Berry, C. L. (1991). Purkinje cell toxicity of beta-aminopropionitrile in the rat. Virchows Arch. A Pathol. Anat. Histopathol. 419, 403-408.

Molnar, J., Fong, K. S. K., He, Q. P., Hayashi, K., Kim, Y., Fong, S. F. T., Fogelgren, B., Szauter, K. M., Mink, M. and Csiszar, K. (2003). Structural and functional diversity of lysyl oxidase and the LOX-like proteins. Biochim. Biophys. Acta 1647, 220-224.

Molnar, J., Ujfaludi, Z., Fong, S. F. T., Bollinger, J. A., Waro, G., Fogelgren, B., Dooley, D. M., Mink, M. and Csiszar, K. (2005). Drosophila lysyl oxidases Dmloxl-1 and Dmloxl-2 are differentially expressed and the active DmLOXL-1 influences gene expression and development. J. Biol. Chem. 280, 22977-22985.

Moore, S. W., Roca-Cusachs, P. and Sheetz, M. P. (2010). Stretchy proteins on stretchy substrates: the important elements of integrin-mediated rigidity sensing. Dev. Cell 19, 194-206.

Morris, P. G. and Abrey, L. E. (2010). Novel targeted agents for platelet-derived growth factor receptor and c-KIT in malignant gliomas. Target. Oncol. 5, 193-200.

Ng, M. R. and Brugge, J. S. (2009). A stiff blow from the stroma: collagen crosslinking drives tumor progression. Cancer Cell 16, 455-457.

Ozawa, T., Brennan, C. W., Wang, L., Squatrito, M., Sasayama, T., Nakada, M., Huse, J. T., Pedraza, A., Utsuki, S., Yasui, Y. et al. (2010). PDGFRA gene rearrangements are frequent genetic events in PDGFRA-amplified glioblastomas. Genes Dev. 24, 2205-2218.

Paszek, M. J., Zahir, N., Johnson, K. R., Lakins, J. N., Rozenberg, G. I., Gefen, A., Reinhart-King, C. A., Margulies, S. S., Dembo, M., Boettiger, D. et al. (2005). Tensional homeostasis and the malignant phenotype. Cancer Cell 8, 241-254.

Paulsson, J., Lindh, M. B., Jarvius, M., Puputti, M., Nistér, M., Nupponen, N. N., Paulus, W., Söderberg, O., Dresemann, G., von Deimling, A. et al. (2011). Prognostic but not predictive role of platelet-derived growth factor receptors in patients with recurrent glioblastoma. Int. J. Cancer 128, 1981-1988.

Pfaffl, M. W., Horgan, G. W. and Dempfle, L. (2002). Relative expression software tool (REST©) for group-wise comparison and statistical analysis of relative expression results in real-time PCR. Nucleic Acids Res. 30, e36.

Ramirez, N. E., Zhang, Z., Madamanchi, A., Boyd, K. L., O'Rear, L. D., Nashabi, A., Li, Z., Dupont, W. D., Zijlstra, A. and Zutter, M. M. (2011). The $\alpha_2\beta_1$ integrin is a metastasis suppressor in mouse models and human cancer. J. Clin. Invest. 121, 226-237.

Rangarajan, R., Gong, Q. and Gaul, U. (1999). Migration and function of glia in the developing Drosophila eye. Development 126, 3285-3292.

Rangarajan, R., Courvoisier, H. and Gaul, U. (2001). Dpp and Hedgehog mediate neuron-glia interactions in Drosophila eye development by promoting the proliferation and motility of subretinal glia. Mech. Dev. 108, 93-103.

Read, R. D., Cavenee, W. K., Furnari, F. B. and Thomas, J. B. (2009). A Drosophila model for EGFR-Ras and PI3K-dependent human glioma. PLoS Genet. 5, e1000374.

Reddy, B. V. V. G. and Irvine, K. D. (2011). Regulation of Drosophila glial cell proliferation by Merlin-Hippo signaling. Development 138, 5201-5212.

Riemenschneider, M. J., Jeuken, J. W. M., Wesseling, P. and Reifenberger, G. (2010). Molecular diagnostics of gliomas: state of the art. Acta Neuropathol. 120, 567-584.

Rosin, D., Schejter, E., Volk, T. and Shilo, B.-Z. (2004). Apical accumulation of the Drosophila PDGF/VEGF receptor ligands provides a mechanism for triggering localized actin polymerization. Development 131, 1939-1948.

Sears, H. C., Kennedy, C. J. and Garrity, P. A. (2003). Macrophage-mediated corpse engulfment is required for normal Drosophila CNS morphogenesis. Development 130, 3557-3565.

Sepp, K. J., Schulte, J. and Auld, V. J. (2000). Developmental dynamics of peripheral glia in Drosophila melanogaster. Glia 30, 122-133.

Shih, A. H. and Holland, E. C. (2006). Platelet-derived growth factor (PDGF) and glial tumorigenesis. Cancer Lett. 232, 139-147.

Silies, M. and Klämbt, C. (2010). APC/C(Fzr/Cdh1)-dependent regulation of cell adhesion controls glial migration in the Drosophila PNS. Nat. Neurosci. 13, 1357-1364.

Silies, M. and Klämbt, C. (2011). Adhesion and signaling between neurons and glial cells in Drosophila. Curr. Opin. Neurobiol. 21, 11-16.

Silies, M., Edenfeld, G., Engelen, D., Stork, T. and Klämbt, C. (2007a). Development of the peripheral glial cells in Drosophila. Neuron Glia Biol. 3, 35-43.

Silies, M., Yuva, Y., Engelen, D., Aho, A., Stork, T. and Klämbt, C. (2007b). Glial cell migration in the eye disc. J. Neurosci. 27, 13130-13139.

Smith-Mungo, L. I. and Kagan, H. M. (1998). Lysyl oxidase: properties, regulation and multiple functions in biology. Matrix Biol. 16, 387-398.

Stork, T., Engelen, D., Krudewig, A., Silies, M., Bainton, R. J. and Klämbt, C. (2008). Organization and function of the blood-brain barrier in Drosophila. J. Neurosci. 28, 587-597.

Stramer, B., Winfield, M., Shaw, T., Millard, T. H., Woolner, S. and Martin, P. (2008). Gene induction following wounding of wild-type versus macrophage-deficient Drosophila embryos. EMBO Rep. 9, 465-471.

Tang, S. S., Trackman, P. C. and Kagan, H. M. (1983). Reaction of aortic lysyl oxidase with beta-aminopropionitrile. J. Biol. Chem. 258, 4331-4338.

Tatenhorst, L., Püttmann, S., Senner, V. and Paulus, W. (2005). Genes associated with fast glioma cell migration in vitro and in vivo. Brain Pathol. 15, 46-54.

Ulrich, T. A., de Juan Pardo, E. M. and Kumar, S. (2009). The mechanical rigidity of the extracellular matrix regulates the structure, motility, and proliferation of glioma cells. Cancer Res. 69, 4167-4174.

Verhaak, R. G. W., Hoadley, K. A., Purdom, E., Wang, V., Qi, Y., Wilkerson, M. D., Miller, C. R., Ding, L., Golub, T., Mesirov, J. P. et al. (2010). Integrated genomic analysis identifies clinically relevant subtypes of glioblastoma characterized by abnormalities in PDGFRA, IDH1, EGFR, and NF1. Cancer Cell 17, 98-110.

Vidal, M. and Cagan, R. L. (2006). Drosophila models for cancer research. Curr. Opin. Genet. Dev. 16, 10-16.

von Hilchen, C. M., Hein, I., Technau, G. M. and Altenhein, B. (2010). Netrins guide migration of distinct glial cells in the Drosophila embryo. Development 137, 1251-1262.

Wang, X., Bo, J., Bridges, T., Dugan, K. D., Pan, T.-C., Chodosh, L. A. and Montell, D. J. (2006). Analysis of cell migration using whole-genome expression profiling of migratory cells in the Drosophila ovary. Dev. Cell 10, 483-495.

Weaver, V. M., Petersen, O. W., Wang, F., Larabell, C. A., Briand, P., Damsky, C. and Bissell, M. J. (1997). Reversion of the malignant phenotype of human breast cells in three-dimensional culture and in vivo by integrin blocking antibodies. J. Cell Biol. 137, 231-245.

Witte, H. T., Jeibmann, A., Klämbt, C. and Paulus, W. (2009). Modeling glioma growth and invasion in Drosophila melanogaster. Neoplasia 11, 882-888.

Wood, W., Faria, C. and Jacinto, A. (2006). Distinct mechanisms regulate hemocyte chemotaxis during development and wound healing in Drosophila melanogaster. J. Cell Biol. 173, 405-416.

Xie, X. and Auld, V. J. (2011). Integrins are necessary for the development and maintenance of the glial layers in the Drosophila peripheral nerve. Development 138, 3813-3822.

DEVELOPMENT

## Supplementary Methods

### Quantitative RT-PCR (qRT-PCR)

For the quantitative RT-PCR we used the following primers:
reaction *lox* (5' GTCTGCGCAGCCCACGGAAA; 3' TACCGGAAGGTGGCCCAGGG), *lox2* (5'
CATTCACATGGCAGATGCGG; 3' GAATCCCACTCGTCATCGCA), *myospheroid* (5'
TGTCGAGCGGATAGCACATC; 3' ACTCGCATGTACCGTGATCG), *Actin5c* (5' GAGCGCGGTTACTCTTTCAC;
3' ACTTCTCCAACGAGGAGCTG), *RpL32* (5' GTTCGATCCGTAACCGATGT; 3'
CCAGTCGGATCGATATGCTAA), *Gapdh1* (5' CGGACGGTAAGATCCACAAC; 3' CCGCCCAGAACATCATCC),
*elav* (5' GCGCACAAACCTTATTGTCA; 3' CGGATTGAGAGGATCGATGT), *EF1*, *Gapdh2*, *alphaTub84B*,
*RpL13A*, *Ef1a48D* and *Hsp70* for SYBR green-monoplex reaction, and
*lox* (Dm02151941_g1; FAM-labeled), *Act5c* (Dm02361909_s1; VIC-labeled) and *RpL32*
(Dm02151827_g1; VIC-labeled) for TaqMan Gene Expression Assays for duplex reaction (Applied
Biosystems).

Human materials were examined with TaqMan Gene Expression Assays (Applied Biosystems) LOX
(Hs00942480_m1), LOXL1 (Hs00173746_m1) and LOXL4 (Hs00260059_m1) and normalized to
glyceraldehyde-3-phosphate dehydrogenase (GAPDH) expression using primers GAPDH-fwd 5'-
ACCCACTCCTCCACCTTTGAC-3', GAPDH-rev 5'-CATACCAGGAAATGAGCTTGACAA-3', and GAPDH-
probe 5'-CTGGCATTGCCCTCAACGACCA-3'. Rat materials were analyzed using LOX
(Rn00566984_m1), LOXL1 (Rn01418038_m1) and LOXL4 (Rn01410863_m1) and normalized to
GAPDH expression using primers GAPDH-fwd 5'-CAAGAAGGTGGTGAAGCAG-3', GAPDH-rev 5'-
CAAAGGTGGAAGAATGGGAG -3' and GAPDH-probe 5'-ACTAAAGGGCATCCTGGGCTACACTGAGGAC-3'.
All experiments were performed in triplicate.

### Immunohistochemistry

Generally, fly specimens were mounted in Vectashield (Vector Laboratories). The following
antibodies were used: Mouse anti-Repo antibodies (1:5) were obtained from the Developmental
Studies Hybridoma bank (Iowa City, IA), anti-Nidogen (1:2,000, gift of S. Baumgartner). Rabbit anti-
GFP (1:1,000, Invitrogen) and goat anti-HRP (DyLight$^{TM649}$ conjugated AffiniPure HRP) (1:500, Dianova
GmbH) and Alexa 488, 568 or 647 (1:1,000, Molecular Probes) ) and biotinylated goat anti-rabbit
secondary antibodies (1:500, Dako) were used as secondary antibodies. Anti-hLOX (1:1,500,
Abnova), anti-hLOXL1 (1:400, Deciphergen Biotechnology), anti-hLOXL4 (1:400, Enzo Life Sciences),
anti-Ki67 (1:100, Acris Antibodies). For mammalian tissue and cells, staining was done using the ABC
method (Vector Laboratories) and sections were counterstained with hematoxylin.
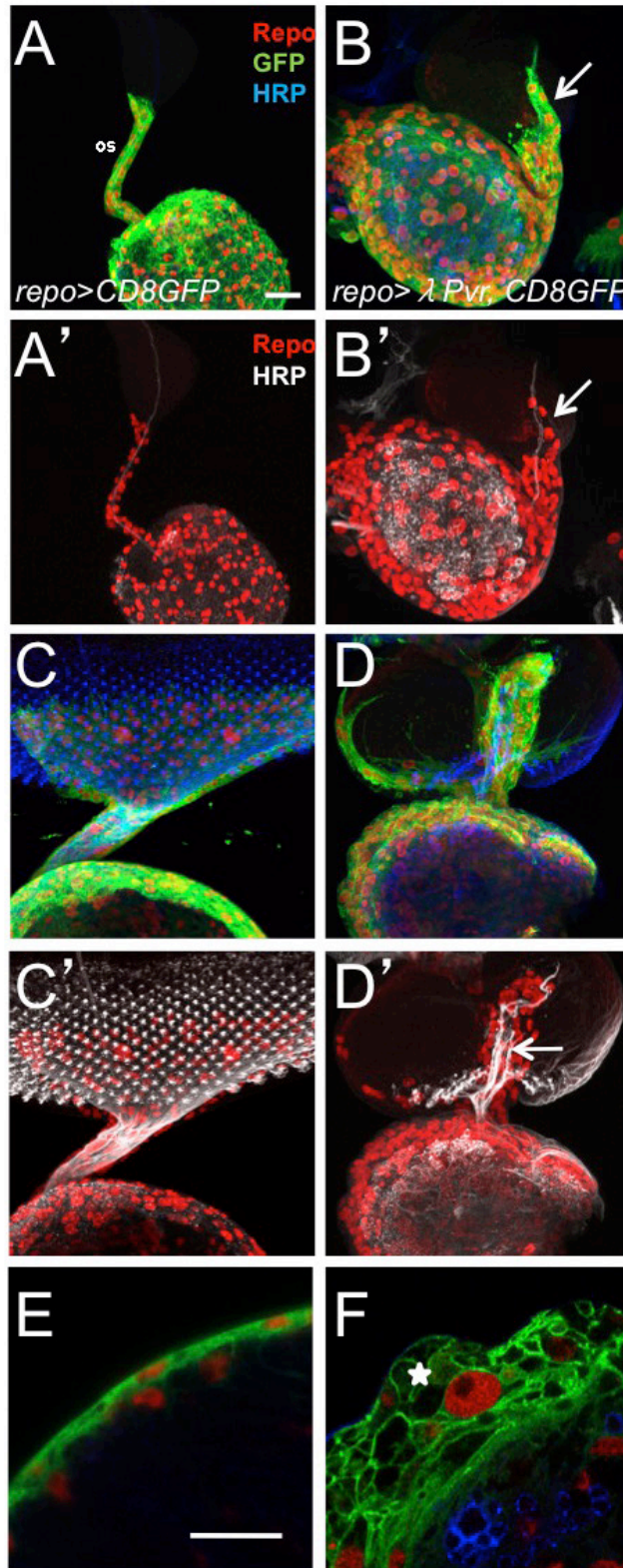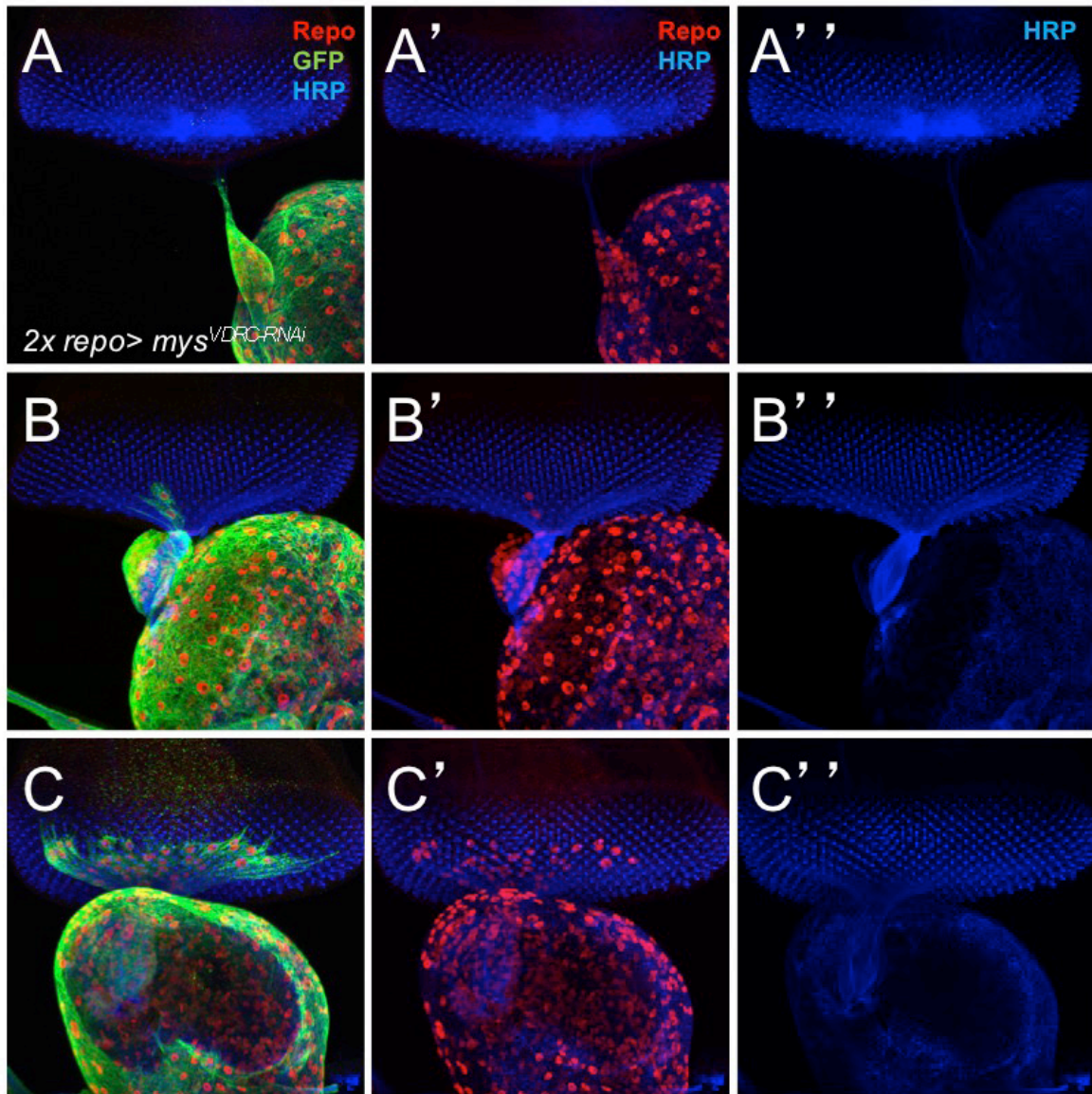
**Supplementary Figure 1. PVR causes early onset of glial migration.** Staining of eye imaginal discs for expression of CD8G-FP specifically expressed by all glial cells (green), Repo protein to highlight all glial nuclei (red), and the HRP antigen which is found on all neuronal membranes (blue or grey). Scale bars are 20 $\mu$m. **A**) Second instar larva. Glial migration onto the eye disc has not yet started. os, optic stalk. **B**) Second instar larva overexpressing activated PVR in all glial cells. The arrow denotes glial cells prematurely migrating onto the eye disc. **A',B'**) Only glial nuclei and neuronal membranes are shown. **C,C'**) Third instar larva. Note that all photoreceptor cells born in the eye imaginal disc project through the optic stalk towards the brain. **D,D'**) Third instar larva overexpressing activated PVR in all glial cells. Ectopic glial migration can be observed. In addition aberrant axonal projections can be seen (arrow). **E,F**) PVR affects surface glia in the brain. **E**) In larvae of the genotype *repo*-Gal4, UAS-*CD8GFP* glial cells show a normal appearance on the brain surface. **F**) Following pan-glial expression of activated PVR a multilayered organization of glial cells is detected and larger glial nuclei are seen (asterisk). Same magnification as in (**E**).
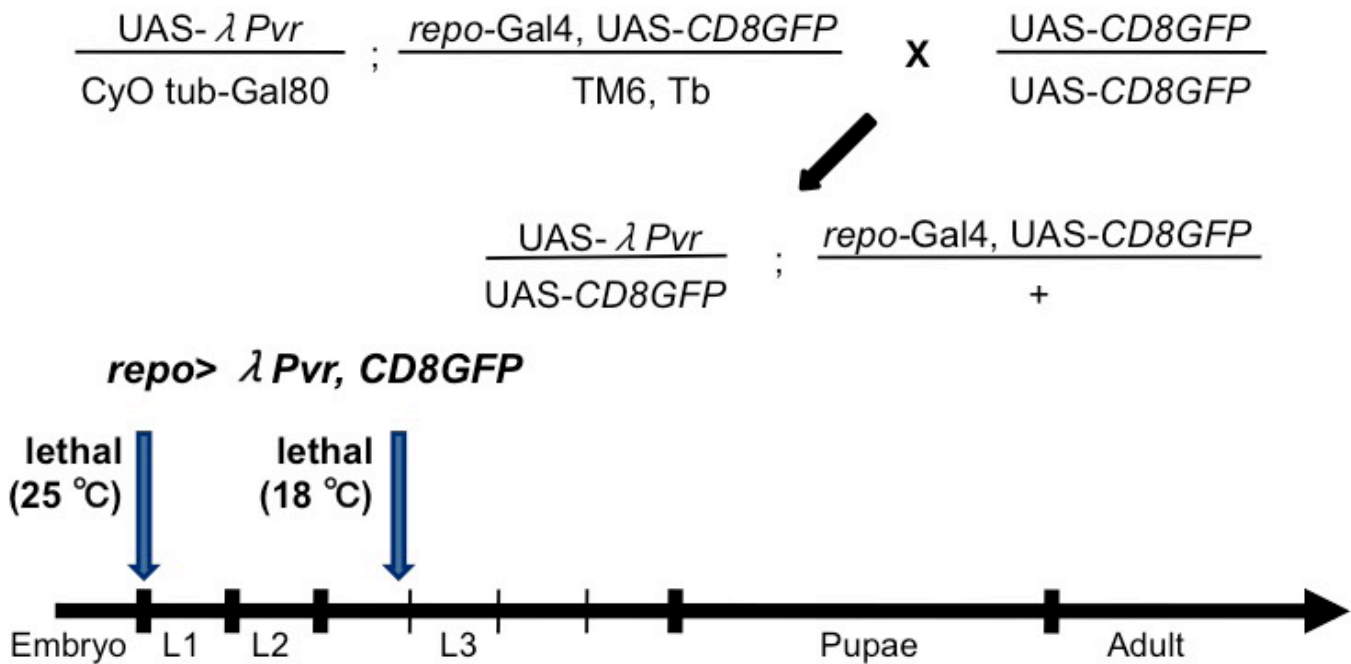
**Supplementary Figure 2. Crossing scheme.** A fly strain with genotype {*UAS-λPvr / CyO tub-Gal80; repo-Gal4 UAS-CD8GFP/TM6 Tb*} was generated. Here no Gal4-mediated expression is observed due to the activity of the Gal80 protein. Upon crossing to flies carrying no Gal80 element all non-TM6 progeny express activated PVR and CD8GFP in all glial cells. Depending on the culture temperature, these flies die as late embryos/early L1 (25°C) or as young L3 larvae (18°C).
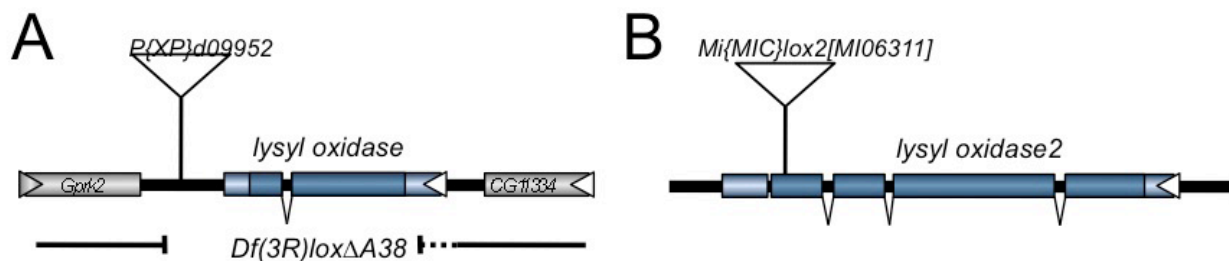


**Supplementary Figure 3. Genomic organization of *lox* and *lox2*. A)** Schematic organization of the Drosophila *lox* gene. The P-element used to generate the small deficiency is indicated. The deletion *Df(3R)lox^{ΔA38}* removes the *lox* gene but leaves the neighboring transcription units intact. **B)** Schematic organization of the Drosophila *lox2* gene. The insertion site of the Minos element close to the LTQ domain is indicated. This insertion likely disrupts the the catalytic function of the Lox2 protein.

**Supplementary Figure 4.** *myospheroid* **affects glial migration onto the eye imaginal disc.** Eye imaginal discs where we suppressed *myosheroid* expression through RNAi were stained for expression of CD8GFP specifically expressed by all glial cells (green), Repo protein to highlight all glial nuclei (red), and the HRP antigen which is found on all neuronal membranes (blue). Upon pan-glial silencing of *myospheroid* three different phenotypic classes were observed. **A)** In the most extreme case, no glial migration onto the eye disc was noted. **B)** In an intermediate class dramatically reduced migration of 10 or less glial cells on the eye disc was noted. **C)** In a third class the number of glial cells moving onto the eye disc was reduced but migration distances appeared relatively normal.

**Table S1. Summary of all AFM measurements**

| Genotype | Number of eye discs | Number of measurements | Median (Pa) | Mean (Pa) | sd | sem |
|---|---|---|---|---|---|---|
| $w^{1118}$ | 10 | 488 | 383.71 | 425.55 | 226.27 | 10.24 |
| $lox^{\Delta A38}$ | 4 | 165 | 221.79 | 221.28 | 89.38 | 6.96 |
| *repo-Gal4>* | 2 | 82 | 335.78 | 356.26 | 163.3 | 18.03 |
| *repo>mycLox* | 4 | 170 | 431.49 | 522.12 | 315.89 | 24.82 |
| *repo>mys$^{dsRNA}$* | 2 | 42 | 183.96 | 210.61 | 100.73 | 15.54 |
| *Fak$^{CG1}$* | 6 | 205 | 177.59 | 327.3 | 332.22 | 23.2 |
| *repo>Integrin* | 7 | 225 | 410.96 | 479.16 | 279.42 | 18.46 |

sd, standard deviation; sem, standard error of the mean. Pa, Pascal.